Transition-metal linkage of antimony-sulfide chains in [M(dien)2] {Sb18S30[M(dien)]2} (M = Mn, Fe, Co)

Article

Accepted Version

Transition-Metal Linkage of Antimony-Sulfide Chains in

[M(dien)$_2$]{Sb$_{18}$S$_{30}$[M(dien)]$_2$} (M = Mn, Fe, Co)

Rachel J. E. Lees,[b] Anthony V. Powell*[a] and Ann M. Chippindale*[a]

Dedicated to Professor A. K. Cheetham FRS, on the occasion of his 70th birthday

Abstract: Three new isostructural transition-metal thioantimonates [M(dien)$_2$]{Sb$_{18}$S$_{30}$[M(dien)]$_2$} (M = Mn (**1**), Fe (**2**), Co (**3**)) have been prepared under solvothermal conditions in the presence of diethylenetriamine (dien). The compounds have been characterised by single-crystal X-ray diffraction, thermogravimetry, elemental analysis, magnetic susceptibility measurements and UV-vis reflectance spectroscopy. The materials crystallise in the space group P-1 and adopt a structure in which complex Sb$_{18}$S$_{30}$$^{6-}$ chains are cross-linked into layers through transition-metal-dimer bridges, [M_2S$_2$], directly bonded to the thioantimonate layers. The layers contain pores, those in successive layers being aligned to generate a channel structure. Additional [M(dien)$_2$]$^{2+}$ cations are located within these channels in the interlayer space.

Introduction

Template-directed synthesis under solvothermal conditions is at the forefront of efforts to create novel materials with interesting electrical, optical and magnetic properties. [1] Originally developed for the laboratory synthesis of zeolitic frameworks, the methodology was extended in 1989 to the preparation of chalcogenides.[2, 3] Subsequently this approach has been applied to a wide range of main-group chalcogenides containing gallium indium, germanium, tin and antimony generally in the presence of linear and branched polyamines as structure directing agents.[3] The methodology has also been extended to ionothermal reactions. [4] Thioantimonates (frequently termed 'antimony(III) sulfides' in the literature) exhibit a particularly rich structural diversity, and can adopt 3-fold and pseudo 4- and 5-fold coordination. [5, 6, 7, 8] The primary building units are generally SbS$_3$$^{3-}$ trigonal pyramids, arising from the stereochemical effect of the lone pair of electrons associated with Sb(III), which can be linked by vertex or edge-sharing to generate a range of discrete

[a] Dr. A.M. Chippindale and Prof. A.V. Powell
Department of Chemistry
University of Reading
Whiteknights,
Reading, Berks RG6 6AD, UK
E-mail: a.m.chippindale@rdg.ac.uk and a.v.powell@rdg.ac.uk
[b] Dr. R.J.E. Lees
Department of Chemistry
Heriot-Watt University
Edinburgh EH14 4AS, UK

Supporting information for this article is given via a link at the end of the document

[9] and extended chain,[10] layered[11] and three-dimensional structures.[12] Recently efforts have focused on exploiting the complementary coordination preferences of different main-group elements to generate novel structures. A wide-range of metal-antimony sulphides in which two or more metals are incorporated into the sulphur-based framework have been prepared.[13, 14, 15, 16] By contrast the introduction of transition-metal cations into solvothermal reaction mixtures containing amines, frequently results in the formation of metal-amino complexes. These can themselves act as structure directing agents, whilst also fulfilling a charge-balancing role. For example cationic tris(ethylenediamine) transition-metal complexes serve to balance the charges of SbS$_2$$^-$ and Sb$_4$S$_7$$^{2-}$ infinite chains in [M(en)$_3$]Sb$_2$S$_4$ (M = Co, Ni, Fe) [10, 17] and [M(en)$_3$]Sb$_4$S$_7$ (M = Co, Ni, Fe) [17,18] respectively, whilst [Ni(terpy)$_2$]$^{2+}$ (terpy = 2,2′:6′,2″-terpyridine) cations fulfil a similar role between Sb$_{10}$S$_{17}$$^{4-}$ layers in [Ni(terpy)$_2$]$_2$[Sb$_{10}$S$_{17}$].[19] This characteristic extends into the rare examples of three-dimensional structures, including [Co(en)$_3$]Sb$_{12}$S$_{19}$, in which the three-dimensional anionic thioantimonate framework contains [Co(en)$_3$]$^{2+}$ cations located within one-dimensional channels[12] and [Ni(aepa)$_2$]Sb$_4$S$_7$ (aepa = N-(aminoethyl)-1,3-propanediamine), which contains cationic nickel complexes located above and below large Sb$_{14}$S$_{14}$ rings.[20]

With the exception of the coinage metals, [6, 13, 21, 22] the direct coordination of transition-metal cations to the primary-bonded thioantimonate network is less common. One strategy which has been applied in an effort to achieve bonding to the main-group-metal sulfide matrix, is to exploit coordinative unsaturation of the transition-metal centre, through the judicious selection of an amine that is unable to fully coordinate the transition-metal cation. Tris(2-aminoethyl)amine (tren) is particularly useful in this respect as it provides only four donor N atoms leaving up to two vacant coordination sites available on the transition metal. Transition-metal-tren complexes are bonded directly to thioantimonate units in the discrete molecular units of [Co(tren)]$_2$Sb$_4$S$_8$ and [Co(tren)]$_2$Sb$_2$S$_5$, in which two [Co(tren)]$^{2+}$ cations are bridged through cobalt-sulfur bonds to Sb$_4$S$_8$$^{4-}$ and Sb$_2$S$_5$$^{4-}$ units,[23] in [Fe(tren)]FeSbS$_4$, in which [Fe(tren)]$^{2+}$ cations are bonded to FeSbS$_4$$^{2-}$ chains [24] and in [Co(tren)]Sb$_2$S$_4$, [25] where [Co(tren)]$^{2+}$ complexes act as pendant groups to thioantimonate layers. Heterocubane-like layers have been reported in (Am)Mn$_2$Sb$_2$S$_5$ (Am = methylamine, ethylamine, diethylenetriamine and 2,2'-bipyridine),[26, 27, 28,29] mixed-metal layers are linked together *via* hydrazine ligands in

Mn$_2$Sb$_4$S$_8$(N$_2$H$_4$)$_2$,[30] whilst [Co(en)$_3$][CoSb$_4$S$_8$] contains both bridging CoS$_4$$^{6-}$ ions and discrete [Co(en)$_3$]$^{2+}$ complexes.[31]

In this paper, we report the synthesis and characterisation of an isostructural series [M(dien)$_2$]{Sb$_{18}$S$_{30}$[M(dien)]$_2$} (M = Mn (**1**), Fe (**2**), Co (**3**)) with a novel structure in which thioantimonate chains are linked together into layers through unusual dimeric [M_2S$_2$] bridges in the presence of discrete [M(dien)$_2$]$^{2+}$ complexes.

Results and Discussion

Compounds (**1**) – (**3**) are isostructural, comprising anionic transition-metal thioantimonate layers, with charge balancing provided by bis-diethylenetriamine transition-metal complexes. The antimony-sulfur layers contain nine crystallographically-distinct antimony atoms. Bond-valence sums are consistent with the presence of antimony in the trivalent state. With the exception of Sb(2) and Sb(5), each antimony atom is coordinated to three S atoms, with Sb–S distances in compound (**1**) in the range 2.399(1) – 2.599(1) Å, typical of trigonal-pyramidal SbS$_3$$^{3-}$ primary building units. Atoms Sb(2) and Sb(5) are each four-coordinate, with two shorter ($\leq$ 2.6 Å) and two longer ($\geq$ 2.70Å) bonds to sulfur, giving rise to an SbS$_4$$^{5-}$ unit with a see-saw like geometry. The "2 + 2" coordination of this type has been observed in a number of thioantimonates and can be considered to be derived from trigonal bi-pyramidal coordination by removal of one equatorial ligand.[6] As is commonly observed in solvothermally-prepared thioantimonates, each antimony atom has additional longer range Sb–S interactions in the range ~2.9 – 3.77 Å *i.e.* within the sum of the van der Waals' radii of the antimony and sulfur atoms.[32] Bonds with Sb–S distances above 3 Å however make only a small contribution to the valence sum (*ca.* 0.2 v.u.) and are not usually considered in structural descriptions. Of the two crystallographically-distinct transition-metal cations, M(1) exists as a discrete divalent complex, coordinated by two diethylenetriamine ligands in a *pseudo*-octahedral geometry with a *meridonal* conformation. The M–N distances in the [M(dien)$_2$]$^{2+}$ complex are similar to those previously reported.[16]

Linkage of three SbS$_s$$^{3-}$ trigonal pyramids through common vertices gives rise to six-membered heterorings of alternating antimony and sulfur atoms, with a chair-like conformation (Figure 1(a)). The resulting Sb$_3$S$_6$$^{3-}$ secondary building unit, termed a semicube, is particularly prevalent in thioantimonate chemistry. However, unusually, in the title compounds a pair of semicubes, formed from Sb(5), Sb(6), Sb(7) and Sb(2), Sb(3), Sb(6), respectively, share a common Sb(6)–S(8) edge to generate a novel Sb$_5$S$_9$$^{3-}$ sofa-like unit (Figure 1(b)). Sulfur vertices associated with the four-coordinate Sb(2) and Sb(5) atoms serve to link each pair of edge-sharing semicubes to a second pair, generated by the center of inversion, creating an Sb$_{10}$S$_{20}$$^{10-}$ unit.(Figure 1(c)) The linking sulfur atoms have one long Sb–S bond to one semicube in an edge-shared pair and a short bond to its partner in the symmetry-related pair. This linkage creates a non-planar Sb$_4$S$_4$ heteroring with a box-like shape. Terminal sulfur atoms of the Sb$_{10}$S$_{20}$$^{10-}$ moiety are shared
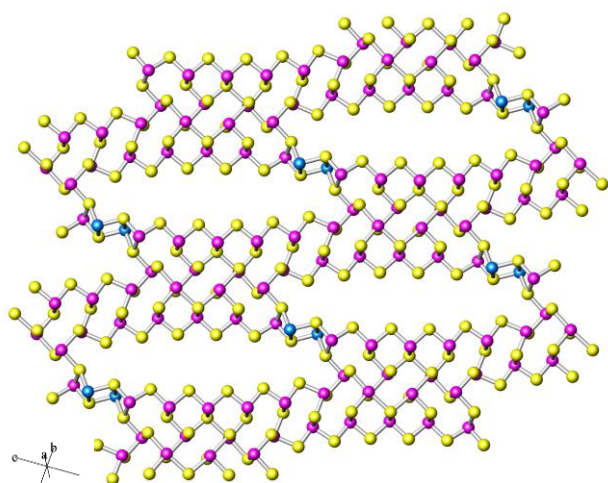
with those of a complex antimony-sulfur unit that contains an Sb$_4$S$_8$$^{3-}$ unit, comprising an Sb$_4$S$_4$ heteroring in a boat-like conformation, with Sb$_2$S$_3$$^{3-}$ side chains attached to each of the two Sb(9) atoms in the ring. This complex unit serves to link the Sb$_{10}$S$_{20}$$^{10-}$ units into zig-zag chains of stoichiometry Sb$_{18}$S$_{30}$$^{6-}$ directed parallel to [01-1]. Sb(1)S$_3$ trigonal pyramids in each chain act are coordinated to a pair of M(1) transition-metal cations, which form a dimeric unit that serves to link the Sb$_{18}$S$_{30}$$^{6-}$ chains into layers parallel to the (110) crystallographic plane (Figure 2). An Sb(1)S$_3$ trigonal pyramid within a given Sb$_{18}$S$_{30}$$^{6-}$ chain acts as a bidentate ligand to one M(2) centre and a monodentate ligand to the second symmetry-related M(2) centre. Thus each of the two M(2) cations are coordinated by three sulfur atoms. The coordination of each M(2) cation is completed by the nitrogen atoms of a dien molecule, giving the cation a *pseudo* octahedral coordination, with the sulfur and nitrogen atoms adopting a *facial* conformation.
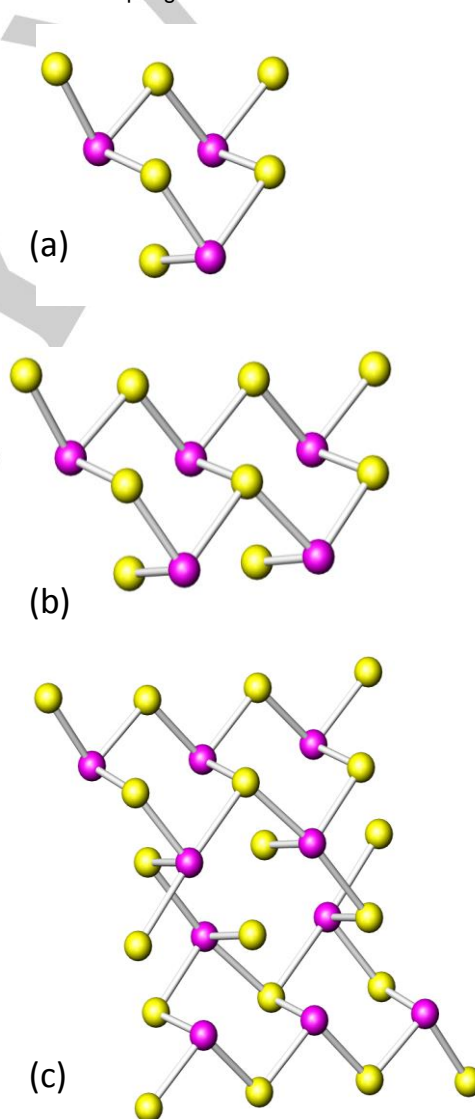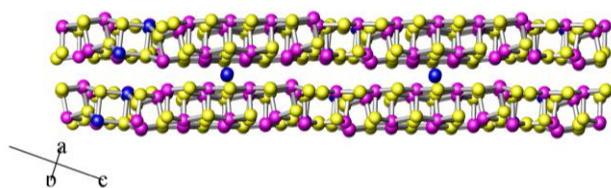

Figure 1. (a) Sb$_3$S$_6$$^{3-}$ semicube comprised of vertex-linked SbS$_3$$^{3-}$ trigonal pyramids. (b) A pair of Sb$_3$S$_6$$^{3-}$ semicubes fused through a common Sb(6)-S(8)

edge to generate a novel $Sb_5S_9^{3-}$ unit. (c) Linkage of $Sb_5S_9^{3-}$ units to generate an $Sb_{10}S_{20}^{10-}$ unit. Key: antimony, magenta spheres; sulfur, yellow spheres.

The linkage through the transition-metal dimer results in negatively charged layers of formula $\{Sb_{18}S_{30}[M(dien)]_2\}^{2-}$. These layers contain large rectangular pores (Figure 2) of approximate dimensions 23 Å × 7.4 Å, defined as atom to atom distances, and are stacked in an *AA* arrangement such that pores in adjacent layers are aligned to form channels directed approximately along the [100] direction. The cationic $[M(dien)_2]^{2+}$ complex formed by the crystallographically distinct *M*(1) cation serves to balance this charge. These complexes are located within the channels at the mid-point between adjacent $\{Sb_{18}S_{30}[M(dien)]_2\}^{2-}$ layers (Figure 3).

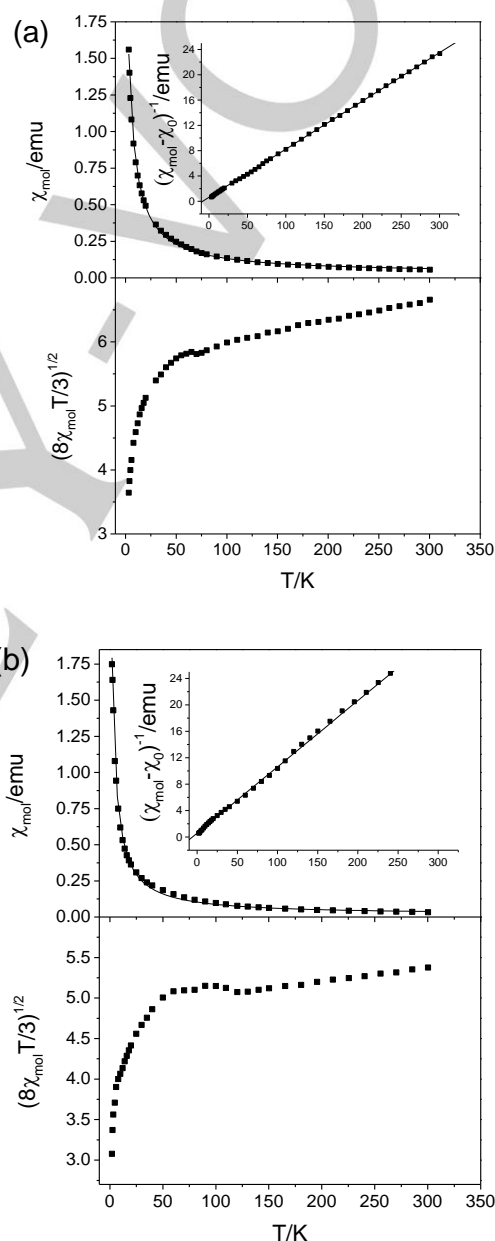**Figure 2.** View of one $\{Sb_{18}S_{30}[M(dien)]_2\}^{2-}$ layer constructed by linkage of $Sb_{18}S_{30}^{6-}$ chains through transition-metal dimers. The large rectangular pores are approximately 23 Å × 7.4 Å. Key: antimony, magenta spheres; sulfur, yellow spheres; blue, transition-metal cation, *M* (2). Carbon, nitrogen and hydrogen atoms are omitted for clarity.

Figure 3. View along [110] of a pair of $\{Sb_{18}S_{30}[M(dien)]_2\}^{2-}$ layers illustrating the $[M(1)(dien)_2]^{2+}$ complexes located in the inter-layer space. Key as in Figure 2.

Magnetic susceptibility data for $[Mn(dien)_2]\{Sb_{18}S_{30}[Mn(dien)]_2\}$ (**1**) and $[Co(dien)_2]\{Sb_{18}S_{30}[Co(dien)]_2\}$ (**3**) exhibit paramagnetic behaviour throughout the temperature range (2 ≤ T/K ≤ 300) and provide no evidence of a long-range magnetic ordering transition (Figure 4). The reciprocal susceptibility data exhibit marked curvature, indicating that the data do not conform to Curie-

Weiss behaviour. Therefore a modified Curie-Weiss expression incorporating a temperature-independent term was fitted to the data over the temperature range 70 – 300 K and 50 – 300 K for compounds (**1**) and (**3**), respectively. Derived magnetic parameters are presented in Table 1. In the case of (**1**), the effective magnetic moment per metal atom (5.91(3)) is in excellent agreement with the spin-only value of 5.92 μ_B for *hs*-Mn^{2+}:d^5, clearly indicating that the transition-metal cation is present in the +2 oxidation state.

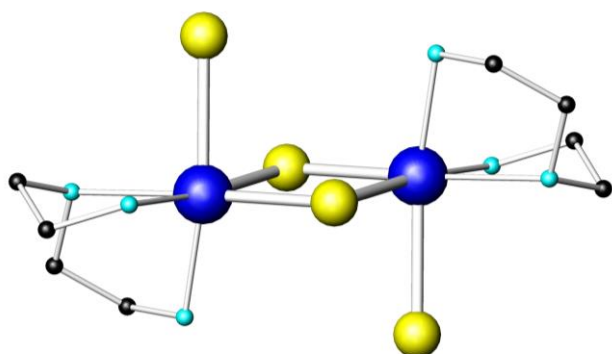
Figure 4. Field-cooled magnetic susceptibility data (upper), inverse susceptibility data (inset), and μ_{eff} as a function of temperature (lower) for (a) $[Mn(dien)_2]\{Sb_{18}S_{30}[Mn(dien)]_2\}$ (**1**) and (b) $[Co(dien)_2]\{Sb_{18}S_{30}[Co(dien)]_2\}$ (**3**). The solid line shows the fit to the modified Curie-Weiss expression described in the text.

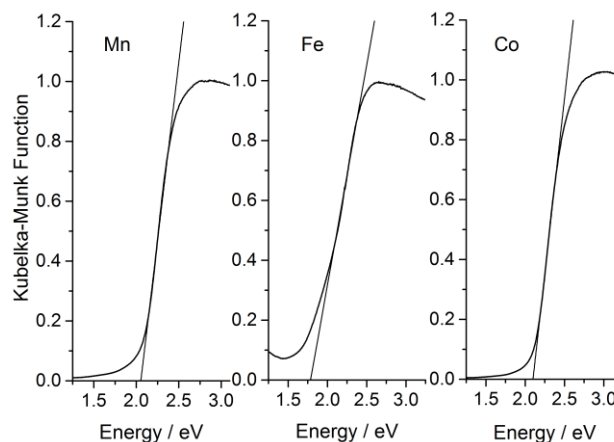**Table 1.** Derived magnetic parameters for $[M(\text{dien})_2]\{Sb_{18}S_{30}[M(\text{dien})]_2\}$

M	Mn (**1**)	Co (**3**)
χ_0 / cm^3 mol^{-1}	1.25(4) ×10^{-2}	3.0(1) × 10^{-3}
C / cm^3 K mol^{-1}	13.1(1)	9.7(3)
θ/ K	-7.9(7)	-1.9(15)
μ_{eff} per M	5.91(3)	5.08(8)

Figure 5. A pair of pseudo-octahedrally coordinated transition-metal (M(2)) cations linked through bridging sulfur atoms, with dien ligands completing the coordination. Key: sulfur, yellow spheres; blue, transition-metal cation, M(2); carbon, black spheres, nitrogen, cyan spheres. Hydrogen atoms are omitted..

The corresponding magnetic moment of 5.08(8) for (**3**) is greater than the spin only value of $\mu_{so} = 3.87$ μ_B for hs-Co^{2+}:d^7, consistent with the expected orbital enhancement associated with the $^4T_{1g}$ ground state of an octahedrally-coordinated d^7 cation.[33] On cooling, the effective magnetic moment of (**1**) decreases from ca. 6.5 to 3.6. Given the absence of an orbital contribution, and hence spin-orbit coupling associated with the $^6A_{1g}$ ground state of octahedral hs-d^5 cations, the reduction in effective magnetic moment of Mn^{2+} appears to be associated with antiferromagnetic correlations. Examination of the structure indicates that the origin of this behaviour lies in the dimeric transition-metal unit (Figure 5). However, the Mn···Mn distance of 3.705(2) Å) is significantly greater than the critical distance identified by Goodenough[34] for direct interaction of metal-based d-orbitals. This suggests that magnetic interactions would occur through a superexchange mechanism *via* the p-orbitals of sulfur. Given that the Mn–S–Mn angles are ~90°, the superexchange interactions are predicted to be antiferromagnetic in origin. However the absence of any ordering transition in the susceptibility data, coupled with the low value of the Weiss constant, suggests the interaction is weak. Although octahedral hs-d^7 cations with ground state $^4T_{1g}$, exhibit spin-orbit coupling, the expected variation in moment is significantly less marked than that observed, suggesting that antiferromagnetic correlations, consistent with a 90° d_σ-p_σ/p_π-d_π interaction, may again be present in the cobalt-containing product. The

magnitude of the Weiss constant suggests that this interaction is also very weak.

Figure 6. Diffuse reflectance spectrum of $[M(\text{dien})_2]\{Sb_{18}S_{30}[M(\text{dien})]_2\}$ (M = Mn, Fe, Co). The solid line shows the extrapolation through the linear portion of the band edge used to determine the band gap.

Diffuse reflectance data are presented in Figure 6. Optical band gaps of 2.05(4), 1.77(3) and 2.10(3) eV were determined for compounds, (**1**), (**2**) and (**3**), respectively. The band gaps are in good agreement with expectations based on the correlation between band gap and framework density that we have previously established for antimony sulphides [15, 35] that is independent of the dimensionality of the thioantimonate structure. Through examination of a large body of experimental data we have shown that there is an approximately linear relationship between the optical band gap and the number of antimony atoms per 1000 Å^3. The origin of this correlation lies in the nature of the electronic states in the vicinity of the Fermi level. In the case of compounds (**1**) to (**3**), there are *ca.* 9.5 Sb atoms per 1000 Å^3. This leads to a predicted band gap of *ca.* 2.0 eV, comparable with the values determined here.

Conclusions

Solvothermal synthesis is well established as a valuable route for the synthesis of metastable thioantimonate structures. This synthetic method continues to generate unusual and original structural motifs, as shown by the new phases presented in this paper. However, the crystallisation process is sensitive to subtle changes in reaction conditions as demonstrated by the fact that the compound [Co(dien)$_2$]{Sb$_{18}$S$_{30}$[Co(dien)]$_2$} (**3**) is formed at 463 K from a reagent mixture of the same composition as that used previously to prepare [Co(dien)$_2$]Sb$_6$S$_{10}$.0.46H$_2$O[36] at 438 K. The structure of the latter consists of Sb$_6$S$_{10}$ $^{2-}$ layers separated by isolated [Co(dien)$_2$]$^{2+}$ cations. Such a dramatic change in crystal structure between the two cobalt-antimony-sulfide compounds suggests that over 25 K, the crystallisation pathway alters significantly. The layered structures of [M(dien)$_2$]{Sb$_{18}$S$_{30}$[M(dien)]$_2$} (M = Mn, Fe, Co), offer rare

examples of structures in which transition-metal ions are bound to a thioantimonate network. In addition, this appears to represent the first example of a thioantimonate in which a dimeric transition-metal unit has been observed within the main-group metal framework. Although the $M \cdots M$ distances (3.705(2) (Mn), 3.648(2) (Fe) and 3.655(2) (Co) Å) exceed the critical distance for direct interaction of cation-based d-orbitals, the evolution of the effective magnetic moment with temperature provides evidence for the existence of superexchange interactions within the transition metal dimer. Optical band gaps in the range 1.77(3) – 2.10(3) eV indicate that the materials are semiconductors and the values are consistent with expectations based on the density of antimony atoms within the structure.

Experimental Section

Synthesis: Single crystals of the title compound, $[M(dien)_2]\{Sb_{18}S_{30}[M(dien)]_2\}$ (M = Mn (**1**), Fe (**2**), Co (**3**)), were prepared under solvothermal conditions in a Teflon-lined stainless steel autoclave with an inner volume of 23 ml.

$[Mn(dien)_2]\{Sb_{18}S_{30}[Mn(dien)]_2\}$ was prepared by heating a mixture of Sb_2S_3 (and MnS with 50% aqueous diethylenetriamine (dien) containing S (0.3 g L^{-1}), with an approximate molar composition Sb:Mn:S:dien of 4:2:6:14, at 438 K for 3.5 days. The solid product was filtered, washed in distilled water then acetone and dried in air at room temperature. The product consisted of large red needles of $Mn(dien)_2\{Sb_{18}S_{30}[Mn(dien)]_2\}$ (**1**), together with a small amount of unreacted Sb_2S_3. CHN analysis of a handpicked sample of $Mn(dien)_2\{Sb_{18}S_{30}[Mn(dien)]_2\}$ found C, 5.39; H, 1.40; N, 4.53% (*calc.* C, 5.15; H, 1.40; N, 4.51%). Thermogravimetric analysis of ~5 mg of handpicked sample using a Du Pont 951 thermal analyser (heating under a flow of dry nitrogen over the temperature range 298-673 K at a rate of 10 $Kmin^{-1}$) showed a single weight loss of 10.58% over the range 578-599 K (SI, Figure S.1), corresponding to complete loss of the organic component (*calc.* 11.06%). Powder X-ray diffraction of the residue showed it to be amorphous.

$[Fe(dien)_2]\{Sb_{18}S_{30}[Fe(dien)]_2\}$ (**2**) and $[Co(dien)_2]\{Sb_{18}S_{30}[Co(dien)]_2\}$ (**3**) were synthesised using FeS and CoS respectively, with the same Sb:M:S:dien molar composition as for $[Mn(dien)_2]\{Sb_{18}S_{30}[Mn(dien)]_2\}$. The mixtures were heated at 463 K for 5 days to form red needles of $[Fe(dien)_2]\{Sb_{18}S_{30}[Fe(dien)]_2\}$ and $[Co(dien)_2]\{Sb_{18}S_{30}[Co(dien)]_2\}$. Powder X-ray diffraction of the solid product indicated the presence of a small amount of unreacted Sb_2S_3 in each product. The iron-containing product also contains FeS and Fe_3S_4 impurities. CHN analysis of handpicked samples of $[Fe(dien)_2]\{Sb_{18}S_{30}[Fe(dien)]_2\}$ and $[Co(dien)_2]\{Sb_{18}S_{30}[Co(dien)]_2\}$ found C, 5.15; H, 1.38; N, 4.28% (*calc.* C, 5.13; H, 1.40; N, 4.49) and C, 5.06; H, 1.34; N, 4.29% (*calc.* C, 5.15; H, 1.40; N, 4.50), respectively. Thermogravimetric analyses showed single-weight losses of 11.49 %, over the range 578-612 K for $[Fe(dien)_2]\{Sb_{18}S_{30}[Fe(dien)]_2\}$ (SI, Figure S.2), and 10.61 %, between 580-611 K for $[Co(dien)_2]\{Sb_{18}S_{30}[Co(dien)]_2\}$ (SI, Figure S.3), which are again consistent with complete loss of the organic components (*calc.* 11.02 and 11.05%, respectively).

Single-crystal X-ray diffraction: Single-crystal X-ray diffraction data for $[M(dien)_2]\{Sb_{18}S_{30}[M(dien)]_2\}$ (M = Mn (**1**), Fe (**2**), Co(**3**)) were measured at 100 K using a Bruker Nonius X8 Apex diffractometer (Mo-K_α radiation (λ = 0.71073 Å)). Intensity data were processed using the Apex-2 software.[37] The structure was solved by direct methods using the program SIR-92,[38] which located all M, Sb and S atoms. Subsequent

Fourier calculations and least-square refinements on F were carried out using the CRYSTALS program suite.[39] The C and N atoms of the amine were located in difference Fourier maps. Hydrogen atoms were placed geometrically on the C and N atoms after each cycle of refinement. In the final cycles of refinement, 358 parameters were refined including positional and anisotropic thermal parameters for all the non-hydrogen atoms. Crystallographic and refinement details are given in Table 2. Crystallographic data (including structure factors) for the structures have been deposited with the Cambridge Crystallographic DataCentre, CCDC, 12 Union Road, Cambridge CB21EZ, UK. Copies of the data for compounds (**1**), (**2**) and (**3**) can be obtained free of charge on quoting the depository numbers CCDC-1507555, CCDC-1507555 and CCDC-1507553, respectively. (Fax: +44-1223-336-033; deposit@ccdc.cam.ac.uk, http://www.ccdc.cam.ac.uk).

Magnetic Measurements: Magnetic susceptibility measurements were performed using a Quantum Design MPMS2 SQUID susceptometer. *Ca.* 10 mg of hand-picked crystals of compounds (**1**) and (**3**) were loaded into a gelatine capsule at room temperature and data were collected over the temperature range ($5 \leq T/$ K ≤ 300) after cooling in the measuring field of 1000 G. Data were corrected for the diamagnetism of the gelatine capsule and for intrinsic core diamagnetism. Crystals of compound (**2**) were coated with an Fe_3S_4 impurity phase. It proved impossible to remove this coating completely by cleaning through suspension in acetone in an ultrasound bath. Since this impurity is ferrimagnetically ordered in the temperature range over which magnetic susceptibility data were collected, it was not possible to measure the intrinsic magnetic properties of (**2**).

Optical Measurements: Diffuse reflectance data were measured over the frequency range 9,090 – 50,000 cm^{-1} using a Perkin Elmer, Lambda 35 UV/Vis spectrometer. $BaSO_4$ was used as a reference material. Measurements were made on *ca.* 10 mg of finely-ground hand-picked crystals of (**1**) – (**3**) diluted with $BaSO_4$. Band gaps were determined by applying the Kubelka-Munk function and extrapolating the linear portion of the absorption edge to the energy axis.[40]

[1]   T. Jiang, A. Lough, G. A. Ozin, R. L. Bedard, R. Broach, *J. Mater. Chem.* **1998**, *8*, 721.

[2]   R. L. Bedard, S. T. Wilson, L. D. Vail, J. M. Bennett, E. M. Flanigen, in *Zeolites: Facts, Figures, Future*, P. A. Jacobs, R. A. van Santen (Eds.), Elsevier, Amsterdam, 1989.

[3]   J. Li, Z. Chen, R. J. Wang, D. M. Proserpio, *Coord. Chem. Rev.* **1999**, *707*, 190.

[4]   W.-W. Xiong, G. Zhang and Q. Zhang, : *Inorg. Chem. Front.* **2014**, *1*, 292.

[5]   W. S. Sheldrick, M. Wachold, *Coord. Chem. Rev.* **1998**, *176*, 211.

[6]   A. V. Powell, *Int. J. Nanotechnol*, **2011**, *8*, 783.

[7]   M. L. Feng, K. Y. Wang, X. Y. Huang, *Chem. Rec.*, **2016**, *16*, 582.

[8]   B. Seidlhofer, N. Pienack, W. Bensch, *Z. Anorg. Allg. Chem.,* **2010**, *65*, 937.

[9]   R. Kiebach, F. Studt, C. Näther, W. Bensch, *Eur. J. Inorg. Chem.* **2004**, 2553.

[10]   R. J. E. Lees, A. V. Powell, A. M. Chippindale, *Polyhedron* **2005**, *24*, 1941.

[11]   R. Stahler, C. Näther, W. Bensch, *Eur. J. Inorg. Chem.* **2001**, 1835.

[12]   P. Vaqueiro, A. M. Chippindale, A. V. Powell, *Inorg. Chem.* **2004**, *43*, 7963.

[13]   K. Y. Wang, M. -L. Feng, X. -Y. Huang, J. Li, *Coordination Chemistry Rev.*, **2016**, *322*, 41

[14]   J. D. Lampkin, A. V. Powell , A. M. Chippindale, *J. Solid State Chem.* **2016**, *243*, 44.

[15]   A. V. Powell and R. Mackay, *J. Solid State Chem.* **2011**, *184*, 3144.

[16]   X. Liu, *Inorg. Chem. Commun.* **2011**, *14*, 437.

[17]   H. O. Stephan, M.G. Kanatzidis, *Inorg. Chem.* **1997**, 36, 6050.

[18]   P. Vaqueiro, D. P. Darlow, A. V. Powell, A. M. Chippindale, *Solid State Ionics*, **2004**, *172*, 601.

[19]   C. Anderer, C. Näther and W. Bensch, *Cryst. Growth Des.* **2016**, *16*, 3802.

[20]   B. Seidlhofer, J. Djamil and W. Bensch, *Cryst. Growth Des.* **2011**, *11*, 5554.

[21]   V. Spetzler, H. Rijnberk, C. Nather, W. Bensch, *Z. Anorg. Allg. Chem.* **2004**, *630*, 142.

[22]   P. Vaqueiro, A. M. Chippindale, A. R. Cowley, A. V. Powell, *Inorg. Chem.* **2003**, *42*, 7846.

[23]   R. Stahler, W. Bensch, *J. Chem. Soc., Dalton Trans.* **2001**, 2518.

[24]   R. Kiebach, W. Bensch, R. D. Hoffmann, R. Pottgen, *Z. Anorg. Allg. Chem.* **2003**, *629*, 532.

[25]   R. Stahler, W. Bensch, *Eur. J. Inorg. Chem.* **2001**, *12*, 3073.

[26]   W. Bensch, M. Schur, *Eur. J. Solid State Inorg. Chem.* **1996**, *33*, 1149.

[27]   M. Schur, C. Nather, W. Bensch, *Z. Naturforsch.* **2001**, *56B*, 79.

[28]   L. Engelke, R. Stahler, M. Schur, C. Nather, W. Bensch, R. Pöttgen, M. H. Möller, *Z. Naturforsch.* **2004**, *59B*, 869.

[29]   C. Anderer, C. Näther and W. Bensch, *Inorg. Chem. Commun.* **2014**, *46*, 335.

[30]   Y. Lu, Y. Tian, F. X. Wei, M. S. C. Ping, C. Huang, F. Boey, C. Kloc, L. Chen, T. Wu and Q. Zhang, *Inorg. Chem. Commun.* **2011**, *14*, 884.

[31]   H.O. Stephan, M.G. Kanatzidis, *J. Am. Chem. Soc.* **1996**, *118*, 12226.

[32]   A. Bondi, *J. Phys. Chem.* **1964**, *68*, 441.

[33]   B.N. Figgis, in *Introduction to Ligand Fields*, Interscience Publishers,New York, **1966**, Chapter 10.

[34]   J. B. Goodenough, in *Magnetism and the Chemical Bond*, , Wiley,New York, **1963**.

[35]   R. J. E. Lees, A. V. Powell, A. M. Chippindale, *J. Phys. Chem. Solids* **2008**, *69*, 1000.

[36]   R. J. E. Lees, A. V. Powell, A. M. Chippindale, *J. Phys. Chem. Solids* **2007**, *68*, 1215.

[37]   Apex-2 Software, Bruker-AXS, Madison, Wisconsin, USA, **2004**.

[38]   A. Altomare, G. Cascarano, C. Giacovazzo, A. Guangliardi, M. Burla, G. Polidori, M. Camalli, *J Appl. Crystallogr.* **1994**, *A27*, 435.

[39]   D. J. Watkin, C. K. Prout, J. R. Carruthers, P. W. Betteridge, CRYSTALS, ISSUE 10, Chemical Crystallography Laboratory, University of Oxford, UK, **1996**.

[40]   W. W. Wendlandt, H. G. Hecht, in *Reflectance Spectroscopy*, Interscience Publishers, New York, **1966**.

Table 2. Crystallographic data at 100 K for [M(dien)$_2$]{Sb$_{18}$S$_{30}$[M(dien)]$_2$} (M = Mn, Fe, Co)
.

	(1)	(2)	(3)
Formula	[Mn(dien)$_2$]{Sb$_{18}$S$_{30}$[Mn(dien)]$_2$}	[Fe(dien)$_2$]{Sb$_{18}$S$_{30}$[Fe(dien)]$_2$}	[Co(dien)$_2$]{Sb$_{18}$S$_{30}$[Co(dien)]$_2$}
M_r	3730.93	3733.69	3742.95
Crystal system	triclinic	triclinic	triclinic
Crystal habit	red needle	red needle	red needle
Crystal dimensions. / mm	0.01 × 0.04 × 0.36	0.01 × 0.02 × 0.40	0.01 × 0.04 × 0.18
Space group	P-1	P-1	P-1
a /Å	7.4142(4)	7.3992(12)	7.3913(5)
b /Å	14.3449(7)	14.357(3)	14.3549(10)
c /Å	18.7996(9)	18.742(3)	18.7340(13)
α /°	74.455(3)	74.377(11)	74.460(4)
β /°	83.385(3)	83.469(9)	83.532(3)
γ /°	86.053(3)	86.008(9)	86.224(3)
V /Å^3	1911.98(17)	1903.3(6)	1901.5(2)
ρ_{calc} /gcm^{-3}	3.240	3.257	3.268
Z	1	1	1
μ /mm^{-1}	7.564	7.673	7.762
Measured data	60327	98248	98882
Unique data	13548	18349	17163
Observed data	8333 ($I \geq 3\sigma(I)$)	9165 ($I \geq 2\sigma(I)$)	9048 ($I \geq 2\sigma(I)$)
R_{int}	0.037	0.063	0.049
$R(F)$	0.0275	0.0410	0.0361
$_wR(F)$	0.0282	0.0390	0.0333

Entry for the Table of Contents (Please choose one layout)

Layout 1:

FULL PAPER

Three new isostructural transition-metal thioantimonates [M(dien)$_2$]{Sb$_{18}$S$_{30}$[M(dien)]$_2$} (M = Mn, Fe, Co) have been prepared under solvothermal conditions in the presence of diethylenetriamine (dien). The structure consists of Sb$_{18}$S$_{30}$$^{6-}$ chains cross-linked into layers through unusual transition-metal-dimer bridges, [M_2S$_2$]. The layers contain pores which align to generate a channel structure in which additional [M(dien)$_2$]$^{2+}$ cations reside.
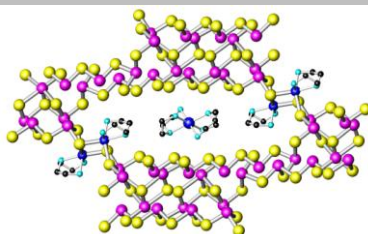
Lee, Powell,* Chippindale*

Page No. – Page No.

Transition-Metal Linkage of Antimony-Sulfide Chains in [M(dien)$_2$]{Sb$_{18}$S$_{30}$[M(dien)]$_2$} (M = Mn, Fe, Co)

Additional Author information for the electronic version of the article.

A.V. Powell: 0000-0002-9650-1568
A.M. Chippindale: 0000-0002-5918-8701